ZONAL DETACHED EDDY SIMULATION (ZDES) FOR INDUSTRIAL AERODYNAMIC FLOWS (ECCOMAS CFD 2010)

Sébastien Deck*

*ONERA-Applied Aerodynamics Department
8, rue des Vertugadins; F-92190 Meudon. France
e-mail: sebastien.deck@onera.fr

Key Words: *Hybrid RANS/LES, Separated Flows, Unsteady, ZDES, DDES, Industrial applications.*

1 Introduction

During the last decades, most of numerical efforts in the field of applied aerodynamics have been focused on the simulation of nominal operational configurations. As a consequence of the rules of design, most practical configurations exhibit only limited separated flow areas and smooth gradients. Therefore, steady methodologies for turbulent flow prediction are able to handle these flowfields with a sufficient degree of accuracy. New industrial needs in aerodynamics concern for example the control of noise as well as the capability to predict the dynamic loads so that the simulation of 3D unsteady turbulent flows is now required. The primary obstacle to practical use of LES on industrial flows which involve wall boundary layers at high Reynolds number remains computational power resources. Indeed LES aims at capturing the scales of motion responsible for turbulence production which imposes severe demands on the grid resolution near solid walls. Hybrid RANS/LES was invented to alleviate this resolution constraints in the near-wall regions. Hybrid methods can be categorized into two major classes corresponding respectively to “weak” and “strong” RANS/LES coupling methods (see figure 1).

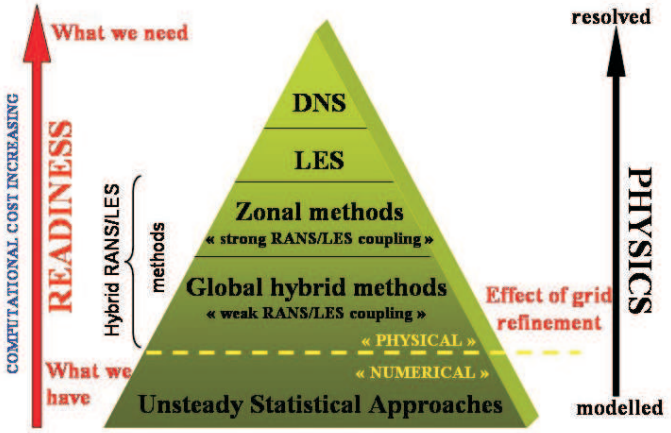

Figure 1: Classification of unsteady approaches according to levels of modelling and readiness (from [1]).

Among these methods, the approach that has probably drawn most attention in the recent time frame is the Detached Eddy Simulation (DES97) which was proposed by Spalart et al.[2]. The idea is to

simulate the attached boundary layer in RANS mode whereas the separated flow should be ideally simulated in LES mode. The methods where the attached boundary layer is modelled is RANS mode can be considered as weak RANS-LES coupling methods since there is no mechanism to transfer the modelled turbulence energy into resolved turbulence energy. These methods introduce a "grey-area" in which the solution in neither pure RANS nor pure LES since the switch from RANS to LES does not imply an instantaneous change in the resolution level. In practice, the eddy viscosity remains continuous across the RANS/LES interface but the rapid decrease of the level of RANS eddy viscosity enables the development of strong instabilities. This family of techniques is well adapted to simulate massively separated flows characterized by a large scale unsteadiness dominating the time-averaged solution (see [1, 3] for further discussion).
Two weaknesses in the use of hybrid methods for technical flows are classicaly identified. The first one concerns a possible delay in the formation of instabilities in mixing layers due to the advection of the upstream RANS eddy viscosity. The second one deals with the treatment of the "grey-area", where the model switches from RANS to LES, and where the velocity fluctuations, the "LES-content", are expected to be not sufficiently developed to compensate for the loss of modelled turbulent stresses. This can lead to unphysical outcomes, like an underestimation of the skin friction.
In order to get rid of this latter drawback, Spalart *et al.*[4] proposed a modification of the model length scale presented as a Delayed Detached Eddy Simulation (DDES) to delay the switch into the LES mode and to prevent "model-stress depletion" (MSD). In a different spirit, Deck[5] proposed a Zonal Detached Eddy Simulation (ZDES) approach, in which RANS and DES domains are selected individually. The motivation is to be fully safe from MSD and GIS and to clarify the role of each region. This raises also the issue of zonal or non-zonal treatment of turbulence.

In addition, "weak-coupling" methods may not be adequate in situations where the flow is sensitive to the history of the upstream turbulence like a shallow separation bubble on a smooth surface induced by a moderate adverse pressure gradient. As a consequence, the simulation has to be fed with turbulent fluctuations to match the low-order statistics given for example by a RANS calculation. In this framework, the hybrid RANS/LES model can be considered as a LES where the RANS model plays the role of a wall-layer model.

In the following, the main features of ZDES are presented as well as recent improvement of the ZDES method including the synthetic reconstruction method for the pseudo viscosity field $\tilde{\nu}$ in the frame of a synthetic eddy method. The objective is to broaden the application area of such hybrid RANS/LES methods by permitting the activation of LES inside the boundary layer. We then focus on a selected number of typical applications of industrial interest studied in the Applied Aerodynamics Department at ONERA.

2 ZDES

2.1 Formulation

The formulas of ZDES differ from those of DES97 or DDES in the definition of the ZDES length scale, the subgrid length scale and the treatment of the near wall dunctions in LES mode. Let us consider a multi-domain mesh made of N blocks and let $ides(ndom)_{1\leq ndom\leq N}$ be a label such as:

$$\begin{aligned} ides\,[ndom] &= 0 \quad if\ domain\ ndom\ is\ in\ RANS\ mode \\ ides\,[ndom] &= 1 \quad if\ domain\ ndom\ is\ in\ DES\ mode \end{aligned} \tag{1}$$

The ZDES length scale becomes:

$$\tilde{d}_{ZDES} = (1 - ides\,[ndom])\,.d_w + ides\,[ndom]\,.d_{DES}^{I\ or\ II} \tag{2}$$

where d_w and $\tilde{d}_{DES}^{I,II}$ denote respectively the distance to the wall and the hybrid length scale which is chosen depending on the problem of interest:
• problem of category I: location of separation fixed by the geometry:

$$\tilde{d}_{DES}^{I} = \min\left(d_w, C_{DES}\Delta\right) \tag{3}$$

• problem of category II: location of separation unknown $a\ priori$:

$$\tilde{d}_{DES}^{II} = d_w - f_d \max\left(0, d_w - C_{DES}\Delta\right) \tag{4}$$

where $f_d = 1 - \tanh\left(\left(8\frac{\nu+\nu_t}{\sqrt{U_{i,j}U_{i,j}\kappa^2 d_w^2}}\right)^3\right)$ is the original DDES function designed to be equal to zero in the boundary layer and 1 elsewhere. Δ is the subgrid length scale which is equal to $\max\left(\Delta x, \Delta y, \Delta z\right)$ when $f_d < 0.8$ and $\left(\Delta x \Delta y \Delta z\right)^{\frac{1}{3}}$ otherwise. This zonal definition of the subgrid length scale Δ has been successfully used in the case of a backward facing step flow[6] and combines the best features of ZDES and DDES.

We also chose to remove the near wall functions in LES mode formulation when $\tilde{d}_{DES}^{I}$ is retained (or when $f_d > 0.8$ when $\tilde{d}_{DES}^{II}$ is retained):

$$f_{v1} = 1 \quad f_{v2} = 0 \quad f_w = 1 \tag{5}$$

RANS mode is the default mode so that the user has to mark only the DES domains. If necessary, the switching into LES mode within a DES domain can be prescribed by the user (for example, if the boundary layer thickness is known). Note also that Eq.(2) can be extended to any RANS model by substituting d_w by the length scale of the underlying turbulence model. Besides, standard DDES can be considered as a particular case of ZDES assuming $ides\,[ndom] = 1$ and $\Delta = \max\left(\Delta x, \Delta y, \Delta z\right)$ everywhere.

As reminded earlier, one of the motivation is to be fully safe from MSD and GIS and to clarify the role of each region. In practice, ZDES switches very quickly to the LES mode, thus limiting the grey area, responsible for the delay in the formation of instabilities. Besides, the interest of this approach is that the user can focus his grid refinement on regions of interest without corrupting the boundary layer properties farther upstream or downstream. As a counterpart, the user decision load is significantly increased compared to an "automatic" approach like DDES

2.2 Stimulated ZDES

The generation of inlet conditions for spatially developing turbulent flows remains one of the challenges that must be addressed prior to the application of LES and hybrid RANS/LES to industrial flows. In the frame of hybrid RANS/LES, the reconstruction of turbulent fluctuations in the outer layer of the boundary layer is of primary importance. A wide range of methods has been developed in the framework of LES and DNS (see the review in [7, 1]) but, as reminded in the introduction, few of them have been

designed to operate in a DES framework where the pseudo-viscosity $\tilde{\nu}$ needs to be reconstructed. An extension of the original SEM method[8, 9] proposed by Pamiès et al.[10] is extended in the framework of a Zonal Detached Eddy Simulation (ZDES)[11]. In the frame of SEM, coherent eddies are randomly generated both in time and space in the inflow plane. Following this principle, a stochastic signal is built for each velocity component and superimposed to a mean. A renormalization condition ensures that the signal has a unit variance. The signal is then linearly transformed to match prescribed Reynolds stresses using a Cholesky decomposition:

$$u_i\left(x,y,z,t\right) = U_i(y) + \sum_j a_{ij}\tilde{u}_j\left(x,y,z,t\right) \quad i = 1,2,3 \tag{6}$$

where the $a_{ij}(y)$ correspond to the Cholesky decomposition of a prescribed Reynolds tensor $R_{ij}(y)$. The eddy viscosity field is then reconstructed from the synthetized velocity field.

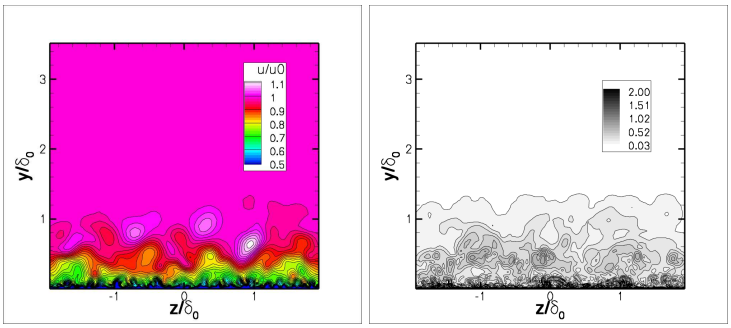

Figure 2: Instantaneous streamwise velocity field (left part) and instantaneous pseudo eddy viscosity field $\tilde{\nu}/\nu$ (right part) in the inlet plane.

Figure 2 presents the contours of the streamwise component of the velocity and pseudo viscosity generated at the inlet. One can notice that the stimulated ZDES method already provides a high degree of realism of the inflow data which helps to speed its achievement up.

3 Example of applications

In this section, we focus on a selected number of typical applications of industrial interest studied in the Applied Aerodynamics Department at ONERA. In the following, the flow configurations are categorized whether the separation location if fixed by the geometry (category I) or a pressure gradient on a smooth surface (category II). In the aformentioned cases, the boundary layer is treated in RANS mode so that flows of category III involve the dynamics of the boundary layer.

3.1 Flows of category I

In many industrial flows, the location of separation is triggered more or less by the geometry. As an example, massive, highly unstable separation occurs in the flow over the afterbody of a launcher where the flow is subject to unsteady three-dimensional phenomena which can result in dynamic loads (also called side-loads) and might disturb the stability of the flight. Moreover, these fluctuations can excite a response of the structural modes called buffeting. As a consequence, a better knowledge of the unsteady flow mechanisms involved in the buffet phenomenon is necessary

for the design of afterbodies of future launch vehicles. Since unsteady loads are difficult to measure experimentally, computational methods are becoming of growing interest in space launcher design.

To get a better knowledge of Ariane 5's base flow, wind tunnel tests were performed in the High Speed Wind Tunnel at NLR on a 1:60 Ariane 5+ launcher model. For further details about experimental set-up and unsteady wall-pressure measurements are given by Geurts[12].
The free-stream Mach number is equal to 0.7 leading to a Reynolds number based on the diamter of the main stage equal to 10^6. The structured multiblock mesh is made up of 162 blocks and is based on an O-H topology to avoid singularity problem near the axis. The use of a ZDES approach allows to limit the total number of points to 22.10^6 since the focus region i.e. LES region) is confined in the base flow area (see figure 3).

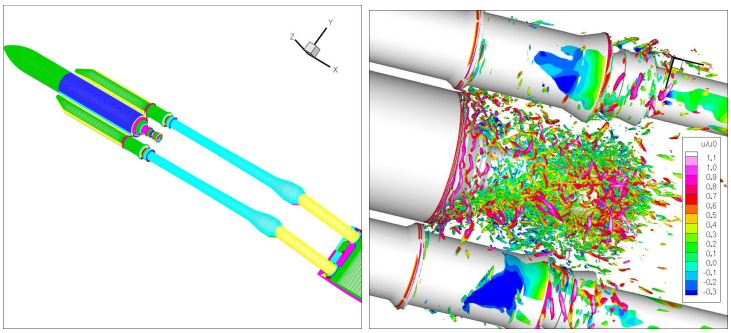

Figure 3: Model (left part) and iso surface of the Q criterion (right part).

Figure 4 compares to the experiment the azimutal evolution of both mean and fluctuating pressure coefficient on the Vulcain2 engine nozzle. The signature of the three-dimensional reattachment of the flow on the Vulcain 2 nozzle is clearly identified and pressure levels are well reproduced by the ZDES. Further investigations in launcher base flow can be found in ref [13, 14].

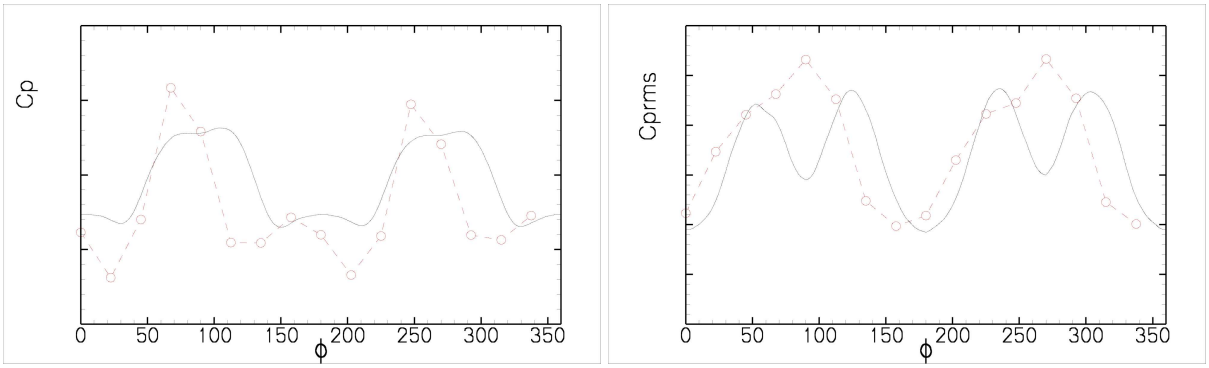

Figure 4: Mean Pressure coefficient (left part) and rms Pressure coefficient (right part).

An other example of flows of category I is provided by an aircraft powerplant configuration at a realistic Reynolds number. This study focuses on the capability of ZDES to accurately simulate a civil aircraft engine jet configuration. Indeed, for the next generation of aircraft projects, the intensity of the interactions between the engine and the airframe could be important and generate critical phenomena. In addition, when the engine is installed closer and closer to the airframe, the evolutions of the interactions are no more linear and it is difficult to extrapolate the actual conventional solutions

in terms of engine installation.

The configuration investigated is a wall-to-wall swept wing equipped with a pylon and an engine. The wing model is representative of the external part of a civil aircraft type wing and was tested in the S3Ch wind tunnel of ONERA during the JEDI project between ONERA and Airbus [15].

The grid used for the present ZDES computations is presented in figure 5 (see Ref [16] for a thorough presentation of the present calculation). It is worth noting that the wing and the engine installation are explicitly treated in RANS mode. The engine jet and wing wake are treated by using the $\tilde{d}^{I}_{DES}$ length scale. The interest of this approach is that the user can focus his grid refinement on regions of interest (e.g. LES regions) without corrupting the boundary layer properties farther upstream or downstream. To avoid a false modelling on the pylon and the plug, the full RANS behaviour is maintained in the ZDES region as long as $d_w < \delta^0_{RANS}$ where δ^0_{RANS} is the boundary layer thickness obtained with the initial RANS calculation. An other calculation employing $\tilde{d}^{II}_{DES}$ is currently under investigation. Patched-grid method is applied in order to perform accurate simulation in ZDES region while limiting the grid density in others RANS regions. Finally a 40 million node grid has been built, most points being clustered in the jet region thanks to an iterative process, based on a RANS - SA results, which objective was to maximize the grid density in the LES regions.

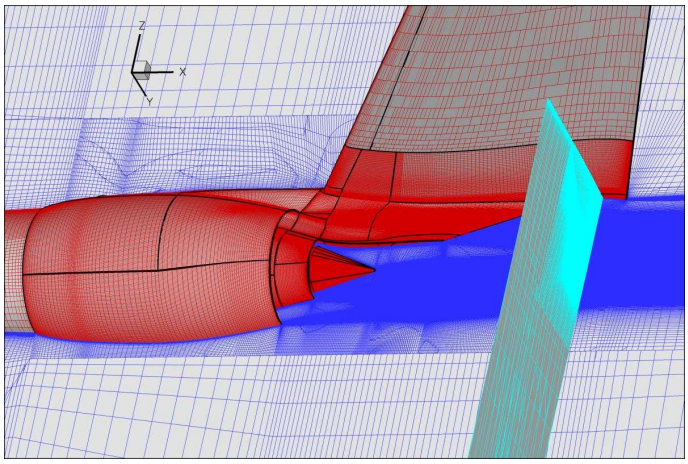

Figure 5: ZDES grid of the engine installation. From [16]

The mixing layers between the fan and core jets as well as the shock in the fan jet are clearly evidenced in the Schlieren type flow visualisation provided in figure 6. The turbulence activity linked to the interaction between the pylon wake and the jet is clearly evidenced as well as the attached boundary layers which are explicitly treated in RANS mode in the ZDES approach. It is worthwhile to notice that there is no delay in the formation of instabilities in the different mixing layers.

The mean and rms velocity profiles at different locations (given in figure 6) are displayed in figure 7. Concerning the mean field, only minor differences are observed between RANS-SA and ZDES. Besides, one can notice the high levels of turbulence coming from the jets inside the engine, caused by the injection system. These experimental turbulence levels inside jets are in the same order of magnitude as the one of the shear layers. Consequently their influence on the diffusion of the jet are probably not negligible. This was not taken into account in this simulation and ongoing work will focus on the coupling of ZDES with a synthetic turbulence generation to mimic the incoming turbulence level.

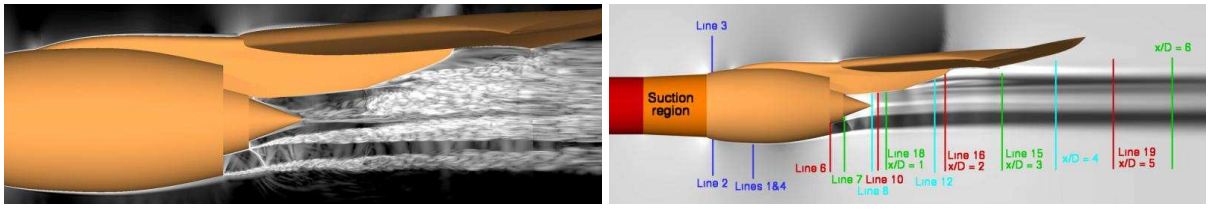

Figure 6: Numerical Schlieren (left part) and rake locations (right part). From [16]

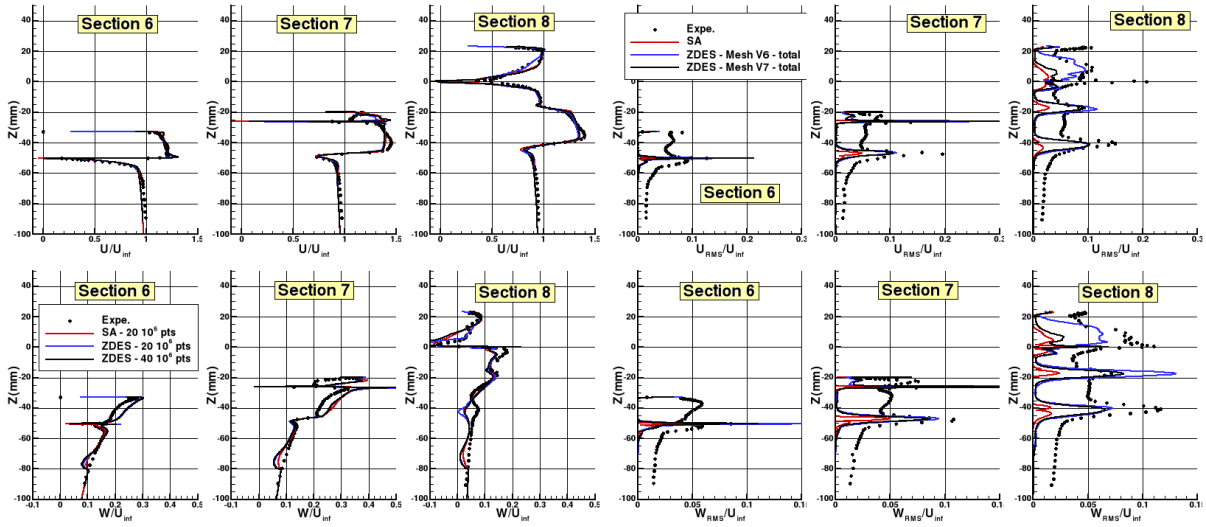

Figure 7: Mean streamwisevelocity profiles (left part) and rms velocity profiles (right part). From [16].

3.2 Flows of category II

In this section, we get interested in flows of category II where the separation is not fixed by the geometry and moves in time so that the d_{DES}^{II} length scale is adopted. Such kind of configurations occur for instance in three-dimensional curved duct. Indeed, let us be reminded that the current trend in the design of missiles or combat aircraft is to enhance the stealth capabilities. Hence the intake integration becomes a more and more important issue. In particular, S-shaped inlets may be beneficial to the reduction of the vehicle size, but are likely to increase the flow distorsion detrimental to the engine performance.

The test case concerns a 3D curved duct investigated in the S19Ch wind tunnel of ONERA. The free stream velocity is equal to 30m/s leading to a Reynolds number base on the step height H equal to $4.1\,10^5$. Further details concerning the experiment investigation can be found in reference [17].

The ZDES grid of the duct is given figure 8. The upstream domain as well as the upper boundary layer are treated in RANS mode. The grid is divided into 20 blocks leading to a total number of $16.5\,10^6$ points. The number of points in the spanwise direction is equal to 194.

Figure 9 shows that the natural grey area defined by $d_w = C_{DES}\Delta$ deeply penetrates in to the boundary layer. The DDES function f_d shields the boundary layer as expected and the present zonal definition of $\Delta = (\Delta x \Delta y \Delta z)^{\frac{1}{3}}$ $(for f_d < 0.8)$ limits significantly the delay in the formation of instabilities.

Figure 10 permits to compare the statistical quantities in the symmetry plane to the available experi-

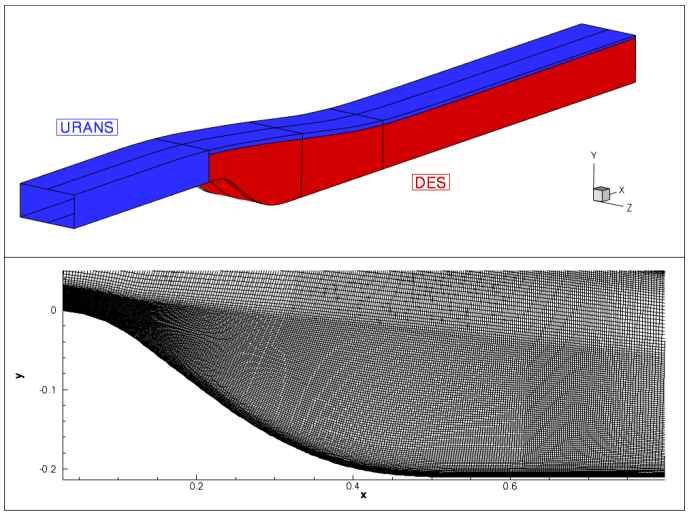

Figure 8: ZDES grid of the curved duct.

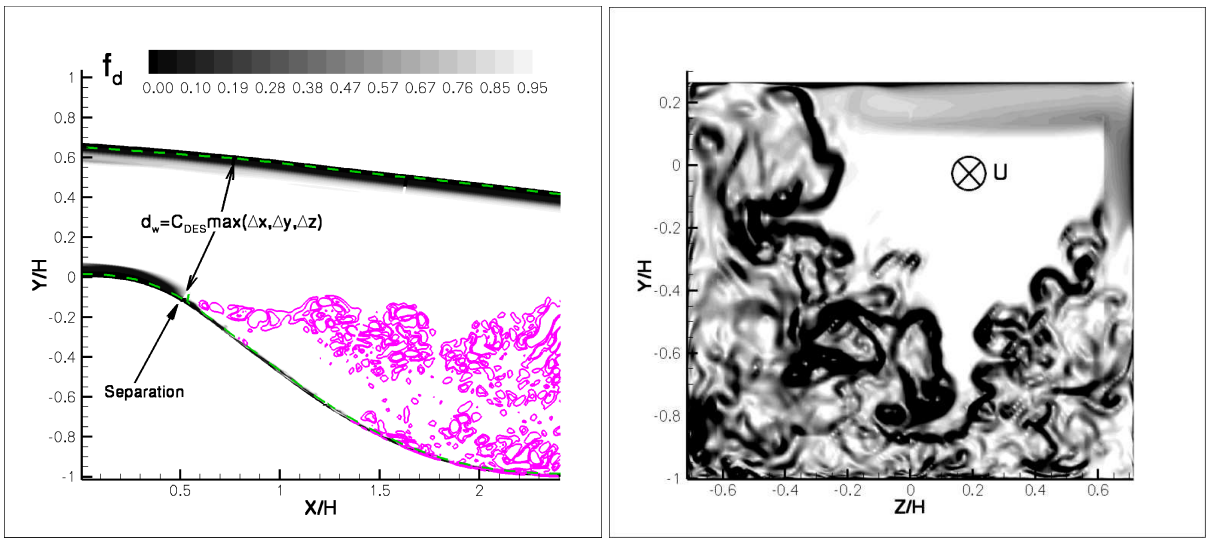

Figure 9: Instantaneous distribution of the f_d function (left part) and instantaneous schlieren in a cross section (right part).

mental data. It is worth noting that the present 3D-RANS calculation does not predict any separation in the plane of symmetry since the corner flow separation are dramatically overpredicted in this case. ZDES improves significantly the prevision of the mean field even if the size of the recirculation bubble is underestimated. The turbulence levels upstream of separation are equal to zero since this region is treated in RANS mode. The turbulence level in the separated area are well reproduced thus permitting to study the dynamic distorsion of the flow in this kind of inlets.

3.3 Flows of category III: Wall turbulence

In the previous applications, the attached boundary layers are systematically treated in RANS mode (natural use of DES-type methods). One of the objective of the present study is to broaden the appli-

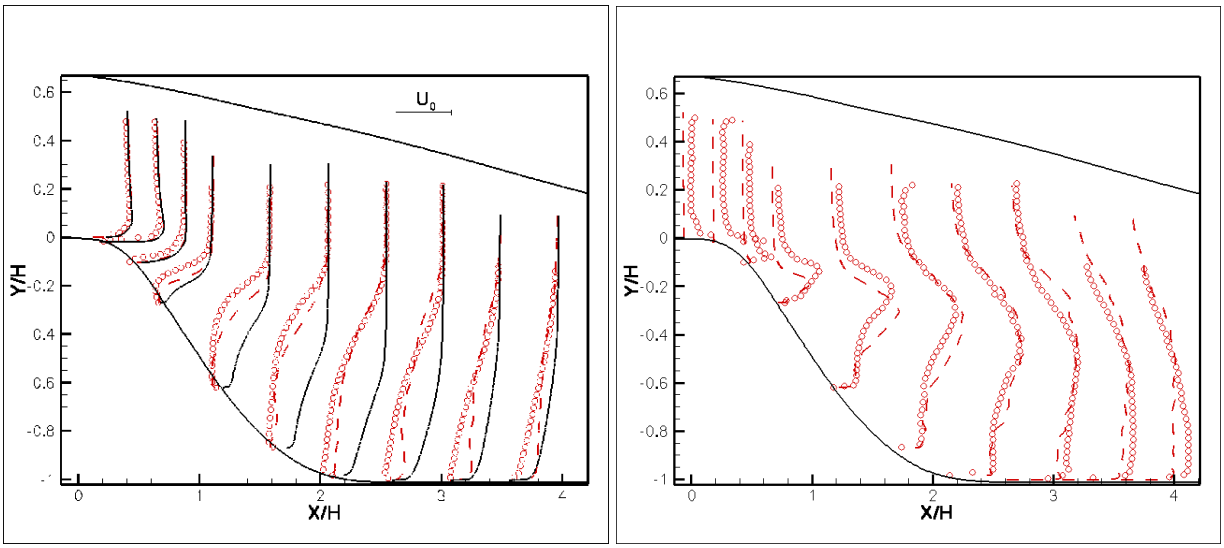

Figure 10: Mean velocity profiles (left part) and turbulence level profiles (right part). Symbol: experiment - solid line : 3D RANS - dashed line : ZDES

cation area of such methods by permitting the activation of LES inside the boundary layer. The zonal aspect of the method ables one to prescribe the RANS interface at a given altitude d_w/δ_0.

The test case is a spatially developing zero-pressure gradient turbulent boundary layer over a smooth flat plate. The free stream velocity is $U_e = 70m.s^{-1}$, the static pressure is set to $P_e = 99120Pa$, the temperature equals $287K$ leading to a Reynolds number per meter $Re = 4.72.10^6 m^{-1}$. The initial boundary layer thickness is $\delta_0 = 3.8mm$ so that $Re_{\delta_0} = 18000$. The Reynolds number based on friction velocity and initial boundary layer thickness (respectively initial momentum thickness) is $Re_\tau = 750$ (respectively $Re_\theta = 1750$).
The computational domain sizes in the streamwise, wall-normal and spanwise directions are respectively $L_x = 62\delta_0$, $L_z = 4\delta_0$ and $L_y = 10\delta_0$ so that the range of Reynolds number covered by the simulation is $1750 \leq Re_\theta \leq 4000$ ($750 \leq Re_\tau \leq 1300$). Note that for $x/\delta_0 > 48$ (where $Re_\theta \approx 3500$), mesh cells are stretched in the streamwise direction so that the turbulent fluctuations are progressively damped. This procedure is common in such simulations and ensures that the outflow condition does not pollute the flowfield in the domain of interest.
The choice of these parameters is motivated firstly by the fact that we want to assess if a turbulent boundary layer can be sustained ($i.e$ without any streamwise artificial relaminarisation) and secondly to evaluate the accuracy of the proposed method by comparing the results with the previously published experimental data by de Graaf and Eaton [18] at $Re_\theta = 2900$. An aditionnal calculation using the mixed scale subgrid model (LES-MSM) is also used for comparison.
An overview of the turbulent content generated by the ZDES simulations is evidenced in figure 11 for several grid resolutions by showing the iso-surfaces of the Q criterion [19] $Q = -1/2\,(||S|| - ||\Omega||)$ with S and Ω denoting respectively the strain and the rotation tensor. It is worth noting that turbulence is sustained in the outer layer even for the coarsest resolutions $\Delta x^+ = 200/\Delta z^+ = 100$ over the whole computational domain. A similar observation has been made by Nikitin et al. [20] with even coarser resolutions in the case of channel flows. However, in the frame of spatially-developing flat plate boundary layer, the unsteady character of the flow field is not imposed by periodic boundary conditions like in channel flows, which makes the present results even more remarkable.

The preponderant terms of the Reynolds stress tensor are then plotted in figure 12 for the finest grid

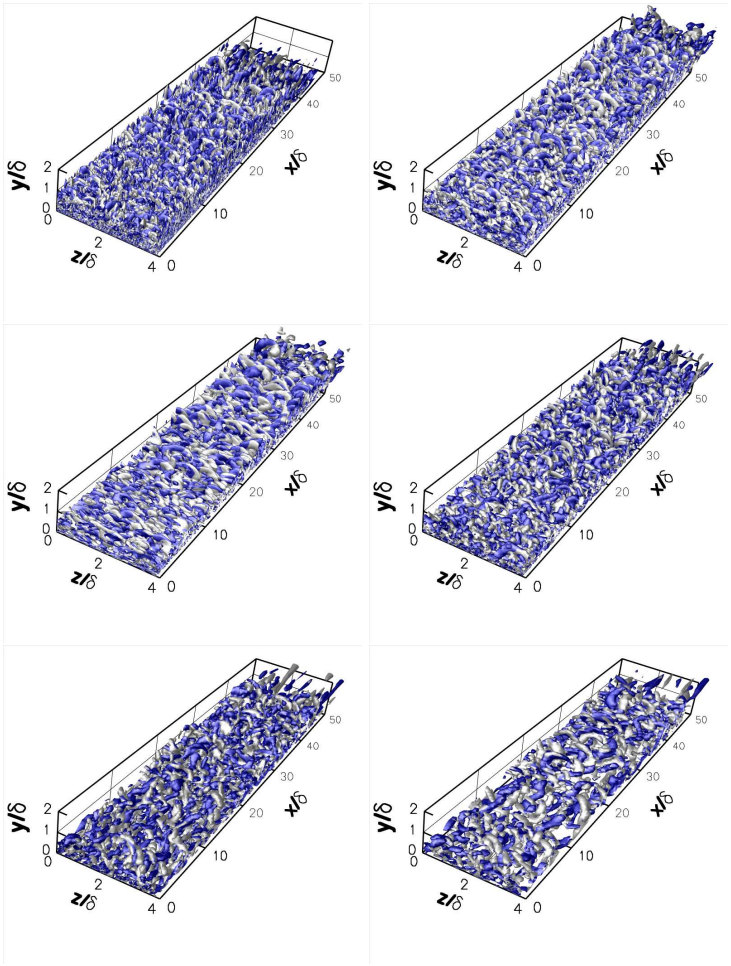

Figure 11: Iso-surface of $QU_e^2/\delta_0^2 = 0.01$: a) 50^+12^+ and 50^+50+ b) 50^+100^+ and 100^+50+ c) 200^+50^+ and 200^+100+.

$\Delta x^+ = 50/\Delta z^+ = 12$. The objective is here to assess the capability of ZDES to deal with wall turbulence like LES with a plausible one-equation SGS model and wall modelling.

As suggested by de Graaf and Eaton [18], the scaling $< u_i^{'} u_j^{'} > \sqrt{Cf/2}$ in mixed-outer coordinates is used. From figure 12, one can notice that all the present calculations ($i.e.$ with the recycling procedure or synthetic turbulence) are in an overall good agreement with the experiments of de Graff & Eaton [18]. However, the behaviors of LES-MSM and ZDES are slightly different depending on the region of the boundary layer. In its inner part, notably, the 15% overestimation of the maximum of streamwise velocity fluctuations by LES-MSM is not present in ZDES calculations. In the outer part of the boundary layer ($i.e$ for $y/\delta > 0.2$), both LES-MSM ans ZDES are hardly underestimating streamwise and wall-normal velocity fluctuations, but the ZDES method succeeds in reproducing the same behavior as LES, which is our target in the frame of a hybrid RANS/LES simulation. The effect of the grid resolution in the frame of ZDES is the subject of ongoing studies at ONERA.

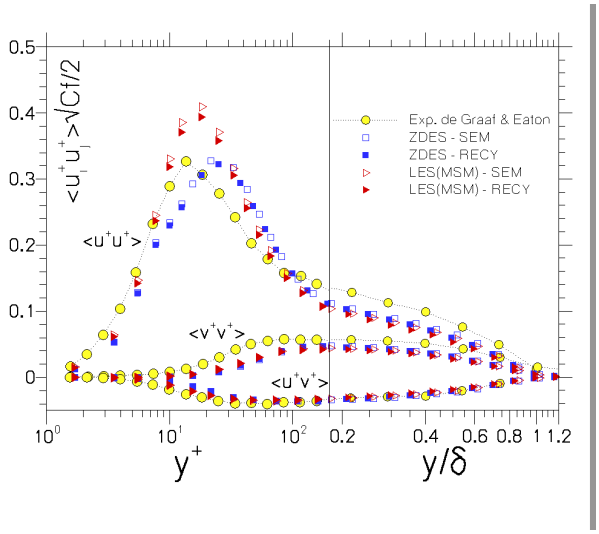

Figure 12: Comparison of the Reynolds stresses between the ZDES results, LES and experimental data at $Re_\theta = 2900$.

4 Concluding remarks

As a conclusion, let us emphasize that even if universal methods for industrial unsteady flows will not be available in the near future, useful results for design and understanding of flow physics can be obtained by adapting the level of modelling to the considered problem without waiting the next generation of supercomputers.

Especially, it has been shown that ZDES offers an already quite interesting domain of application. In this approach, the user defines manually the flow regions in which a RANS or a LES behavior of the algorithm is expected thus allowing to reduce the cost of the simulation by limiting the extent of the LES zones while maintaining the desired level of accuracy in (U)RANS and focus regions. With this approach, the grid refinement is focused on regions of interest (e.g. LES regions) without corrupting the boundary layer properties farther upstream or downstream. Besides, the zonal formulation of the hybrid length scale $\tilde{d}$ allows to combine the zonal approach with the best features of DDES by limiting the delay in the formation of instabilities. In other words, the presumed weak point of a zonal approach, namely that the location of separation has to be known in advance, is now overcome. An improved synthetic eddy method has also been adapted to define an unsteady eddy viscosity which allows to broaden the application area of such hybrid RANS/LES methods by permitting the activation of LES inside the boundary layer.

Whether the treatment of turbulence has to be zonal or not is still an open question. This question has not to be confused with the use of structured and non-structured codes. The author promotes the use of a zonal treatment of turbulence to handle complex configurations because hybrid RANS/LES is primarily an LES except on the wall and a “black-box push-button” method is perhaps not a desirable option. The zonal approach allows also flexibility in the numerics. In a near future, the activation of LES in a boundary layer embedded in an industrial configuration will necessarily be located and thus zonal. Other authors [21] may differ but debate is useful. Both zonal and non-zonal methods will probably

grow and this competitiveness should be mutually beneficial.

REFERENCES

References

[1] P. Sagaut, S. Deck, and M. Terracol. Multiscale and Multiresolution Approaches in Turbulence. *Imperial College Press, London, UK, 356 pages*, 2006.

[2] P. Spalart, W.H. Jou, M. Strelets, and S.R. Allmaras. Comments on the feasibility of LES for wings and on a hybrid RANS/LES approach. *In Proceedings pp 137-147, 1st AFSOR Int. Conf. on DNS/LES, Ruston*, 1998.

[3] J. Frohlich and D. von Terzi. Hybrid RANS/LES methods for the simulation of turbulent flows. *Progress in Aerospace Sciences, 44: 349-377*, 2008.

[4] P.R. Spalart, S. Deck, M.L Shur, K.D. Squires, M. Strelets, and A. Travin. A New Version of Detached-Eddy Simulation, Resistant to Ambiguous Grid Densities. *Theoretical and Computational Fluid Dynamics, Vol 20, pp 181-195, July 2006*, 2006.

[5] S. Deck. Zonal-Detached Eddy Simulation of the Flow around a High-Lift Configuration. *AIAA Journal, vol 43., No. 11, pp 2372-2384*, 2005.

[6] J. Riou, E. Garnier, S. Deck, and C. Basdevant. Improvement of Delayed-Detached Eddy Simulation Applied to Separated Flow over Missile Fin. *AIAA J. ,vol 47, No. 2, pp 345-358*, 2009.

[7] A. Keating, U. Piomelli, E. Balaras, and H.J. Kaltenbach. $apriori$ and $aposteriori$ tests of inflow conditions for large-eddy simulation. *Physics of Fluids, vol.16, No. 12, pp 4696-4712*, 2004.

[8] N. Jarrin, S. Benhamadouche, D. Laurence, and R. Rosser. A Synthetic-Eddy-Method for generating inflow conditions for Large Eddy Simulation. *International Journal of Heat and Fluid Flows, Vol.27, pp 585-593*, 2006.

[9] N. Jarrin, J.-C. Uribe, R. Prosser, and Laurence D. Synthetic Inflow conditions for Wall Bounded Flows. *Advances in Hybrid RANS-LES Modelling, NNFM97, pp 77-86, edited by S-H Peng and W. Haase, Springer-Verlag, Berlin Heidelberg*, 2008.

[10] M. Pamiès, P.E. Weiss, E. Garnier, S. Deck, and P. Sagaut. Generation of synthetic turbulent inflow data for large eddy simulation of spatially evolving wall-bounded flows. *Physics of Fluids, vol 21, 045103*, 2009.

[11] S. Deck, P.E. Weiss, M. Pamiès, and Garnier E. On the use of Stimulated Detached Eddy Simulation for spatially developping boundary layers. *Advances in Hybrid RANS-LES Modelling, NNFM97, pp 67-76, edited by S-H Peng and W. Haase, Springer-Verlag, BerlinHeidelberg* , 2008.

[12] E.G.M. Geurts. Steady and unsteady pressure measurements on the rear section of various configurations of the Ariane 5 launch vehicle. *6th International Symposium on Launcher Technologies, Munich, Germany, November*, 2005.

[13] S. Deck and P. Thorigny. Unsteadiness of an axisymmetric separating flow. *Physics of Fluids, 19, 065103*, 2007.

[14] P.E. Weiss, S. Deck, J.C. Robinet, and P. Sagaut. Dynamics of a turbulent axisymmetric separating/reattaching flow. *Physics of Fluids, 21, 075103*, 2009.

[15] V. Brunet, P. Molton, H. Bezard, and S. Deck. Advanced Experimental and Numerical Investigations of an Aircraft Powerplant Configuration. *27th AIAA Applied Aerodynamic Conference, San Antonio, AIAA paper 2009-4117*, 2009.

[16] V. Brunet and S. Deck. Zonal Detached Eddy Simulation of a civil aircraft engine jet configuration . *3rd Symposium on Hybrid RANS/LES methods, 10/12 June 2009, Gdansk, Poland. To appear in Advances in Hybrid RANS-LES Modelling, Springer-Verlag, Berlin Heidelberg*, 2009.

[17] B. Gardarin, L. Jacquin, and P. Geffroy. Flow separation control with vortex generators. *AIAA Paper 2008-3773, 37th AIAA Fluid Dynamics Conference, Washington, June*, 2009.

[18] D.B. DeGraaf and J.K. Eaton. Reynolds number scaling of the flat-plate turbulent boundary layer. *Journal of Fluid Mechanics, vol 422, pp 319-346*, 2000.

[19] J. Jeong and F. Hussain. On the identification of a vortex. *Journal of Fluid Mechanics, vol.285, pp 69-94*, 1995.

[20] N.V. Nikitin, F. Nicoud, B. Wasistho, K.D. Squires, and P.R. Spalart. An approach to wall modeling in large eddy simulation. *Physics of Fluids, vol.12, pp 1629-1631*, 2000.

[21] P.R. Spalart. Detached eddy simulation. *Annual Review of Fluid Mechanics, 41:181-202*, 2009.